Introduction

Rare earth doped fiber lasers and amplifiers offer a variety of applications in solid-state physics, biophysics, metrology, sensors, photochemistry, medical sciences, and telecommunications, as well as in fundamental research.

Fiber lasers have the big advantage that the guided pump power in the fiber is used with high efficiency due to small core diameter especially in single mode fiber, which leads to strong absorption of the pump power compared to conventional solid-state lasers. Moreover, it is easier to achieve high laser power compared to conventional crystal lasers which need tight focusing in the laser cavity. Furthermore, fiber lasers are small, flexible and robust.

Upconversion fiber lasers may provide a useful route to the development of visible lasers pumped in the near infrared region of the spectrum. The emission wavelength of a fiber laser can be chosen by suitable doping with one or several rare earth ions and additionally adjusted by varying the glass composition. Due to the lower phonon energy of fluoride glasses, they are transparent in a wide wavelength range which makes them a good choice as host material for rare earth elements. In practice, ZBLAN glass based on zirconium fluoride is the most famous type, due to its stable structure. Praseodymium doped ZBLAN fibers offer possible laser transitions in the blue, green, orange and red operating at room temperature. But only additional doping with ytterbium allows to use these laser transitions with just one pump wavelength, which can be delivered by a small and cheap laser diode.

A serious problem with these lasers is the connection between the silica and fluoride fiber due to the large difference in the melting temperature for both of the fibers. Therefore, we have invented a new thermal splicing method to solve this problem. But a high degree of manual control makes this method inaccurate and very difficult to get the same results with each thermal splice. This problem could be avoided by using an automatic control to start and stop the heating process, which was not possible in our current work. For this reason, we improved the glue splice method, which was developed by M. Kozak, to be more robust and flexible. Moreover, a new type of glue splices with gel was created to avoid the Fresnel reflection at the fiber/fiber interface.

In the past years, T. Baraniecki, H. Shalibeik and others at the IHF were working on fiber lasers in the visible spectral range. In this work we have focused our attention on the red and orange lasers with maximized output power in the output fiber of a linear or ring fiber laser setup, without free space parts. We have also improved the tunable fiber laser to get a fiber output power of about 20 and 10 mW in the red and orange range, respectively. Again there was no free space component except of the grating block.

We will divide our work in six chapters, and a short description of their contents will be given below.

Chapter 1: This chapter summarizes the fundamentals of fiber optics, in addition to a short overview on different host materials for rare earth elements. Furthermore general loss mechanisms of optical fibers are described here.

Chapter 2: The most important energy transitions in rare earth ions as well as energy transfer mechanisms and upconversion processes are discussed in this chapter. The upconversion pumping process in praseodymium ions as well as the avalanche upconversion pumping scheme of Pr^{3+}/Yb^{3+}-doped ZBLAN glass are described in details. Finally, the frequency transfer function method is presented and applied to measure the fluorescence lifetimes of level $^1G_4$ in Pr^{3+} and in Pr^{3+}/Yb^{3+}-doped ZBLAN glass, as well as the upper laser level in ytterbium doped ZBLAN glass.

Chapter 3: This chapter starts with a description of splice processes between same and different types of silica fibers, then the differences regarding mechanical and thermal properties of fluoride and silica glasses are discussed to find a new thermal splice method between these different fibers. Although this method was successful, some serious problems could not be solved. Therefore, we developed a glue splicing technique, which is more stable and robust. Moreover, the Fresnel reflection at the fiber/fiber interface was suppressed by addition of gel during the glue splice fabrication. This new method of glue splicing is easier to fabricate than the previous method described by M. Kozak.

Chapter 4: Fiber couplers are important components in the fiber laser setups. Therefore, in this chapter we describe the fabrication method of fiber couplers like wavelength-division-multiplexing (WDM) couplers for pump and signal wavelength. Then the results of all-fiber laser measurements using thermal and glue splices to connect fluoride and silica fibers are presented. Different fluoride fiber lengths are used to find the optimum Pr^{3+}/Yb^{3+}-doped ZBLAN fiber

lengths and the optimum loop mirror reflectivity for the red fiber laser. Moreover, we present a tunable fiber laser in the red range using a thermal splice.

Chapter 5: Here the results of red fiber lasers in linear and ring configuration. But FC/PC connectors were used to connect fluoride and silica fibers. Some of our results are compared with theoretical calculations.

Chapter 6: We concentrate in this chapter on the tunability of Pr^{3+}/Yb^{3+}-doped ZBLAN fiber lasers. Since the obtained laser output power using a single fluoride fiber was low, two fluoride fibers were combined in one setup. As a result the fiber output power was more than doubled. The orange-red tunable fiber laser is also described here in two fiber laser setups. Moreover, the total output power for different fiber output mirror reflectivities is compared to find the optimum reflectivity giving the largest output power.

1 Structure and Properties of Silica and Fluoride Glass Fiber

This chapter will provide fundamental information about the optical fiber. But before going in the fiber properties, we will concentrate on the difference between the silica glass structure and the other host material specially ZBLAN glass, which was used in our work. Furthermore, the reason why the use of fluoride glass fiber as a host material of rare earth elements was indicated here.

1.1 Optical fiber fundamentals

The optical fiber consists of two concentric layers. The inner layer is the light-carrying part called the core, and the surrounding cladding provides the difference in refractive index that allows total internal reflection of light through the core. In general, the refraction index of the cladding is less than 1 % lower than that of the core, to achieve the total internal reflection. This difference must be carefully controlled to obtain desired fiber characteristics.

To protect fibers from the ambient conditions an additional coating is added around the cladding. The coating, which is usually one or more layers of polymer, might affect the physical properties on the fiber. But it has no optical properties affecting the propagation of light within the fiber.

Light injected into the fiber and striking the core-to-cladding interface at greater than the critical angle reflects back into the core. Since the angles of incidence and reflection are equal, the reflected light will again be reflected. The light will continue to be totally reflected and will zigzag down along the length of the fiber. But light striking the interface at less than the critical angle passes into the cladding, where it is lost over distance.

An important parameter of the fiber is the numerical aperture (*NA*), because it gives an indication of how the fiber accepts and propagates light. A fiber with a large *NA* accepts light well; a fiber with a low *NA* requires highly directional light.

The *NA* relates to the refractive indices of the core and cladding, also defines the angles at which rays will be propagated in the fiber. These angles form an

acceptance cone that gives the maximum angle of light acceptance, as given in following equation:

$$NA = \sqrt{n_1^2 - n_2^2} = \sin\theta,$$

where θ is the half-angle of acceptance, and n_1 and n_2 are refractive indices of core and cladding, respectively, see figure 1.1. This angle is zero in a single mode fiber for the guided wave.

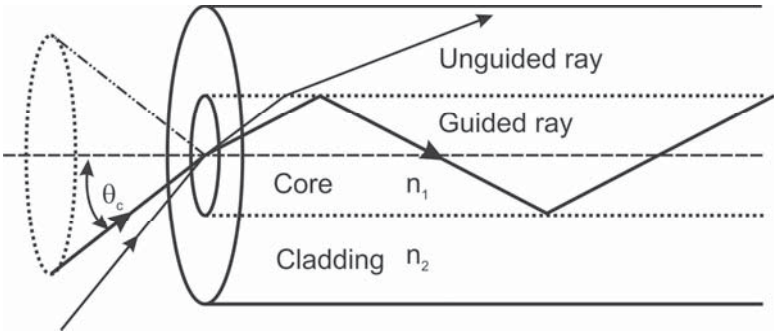

Figure 1.1: The schematic structure of light flowing in a multimode optical fiber

Optical fibers can support a number of guided waveforms called modes. The number of modes in fiber can be calculated from the normalized frequency *V*. For simple step-index fiber, the number of modes can be approximated by [1]:

$$N = \frac{V^2}{2},$$

where the normalized frequency *V* is a fiber parameter that takes into account the core diameter *d*, wavelength propagated λ and fiber *NA*, as following:

$$V = \frac{2\pi d}{\lambda} NA$$

The equations demonstrates that the number of modes is determined by core diameter, fiber *NA*, and the wavelength propagated. When *V*<2.405 the fiber supports a single mode in two polarization, and all higher modes are cut off. The *V* number can be decreased by decreasing the core diameter, by increasing the operating wavelength, or by decreasing the *NA*. Thus, single-mode operation in a fiber can be obtained by suitably adjusting these parameters. The fundamental mode has a bell-shaped spatial distribution similar to Gaussian distribution. This mode provides the highest confinement of light power within the core [2].

1.2 Glass structure and host materials

Glasses are an important class of host material for some of rare earths elements. We start with the simplest glass structure of SiO_2 to understand the difference between glass compositions. Figure 1.2 shows SiO_2, which is formed by strong, directional covalent bonds, and has a well-defined local structure: four oxygen atoms are arrayed at the corners of a tetrahedron around a central silicon atom.

The tetrahedrons are joined to each other with vertices and form the spatial structure, where each oxygen atom belongs to two silicon atoms. This structure is characterized by its small ions, which are located relatively far from each other. It has been mentioned that noncrystalline solids lack a systematic and regular arrangement of atoms over relatively large atomic distances. These materials are sometimes called supercooled liquids, inasmuch as their atomic structure resembles that of a liquid.

Solid forms depend on the ease with which a random atomic structure in the liquid can transform to an ordered state during solidification, whether a solid is crystalline or amorphous. Therefore, amorphous materials are characterized by atomic or molecular structures that are relatively complicated and comparatively open (i.e. the atoms are not closely packed together) either and it becomes ordered only with some difficulty. Moreover, rapidly cooling through the freezing temperature favors the formation of a noncrystalline solid, since only a short time is not allowed for the ordering process.

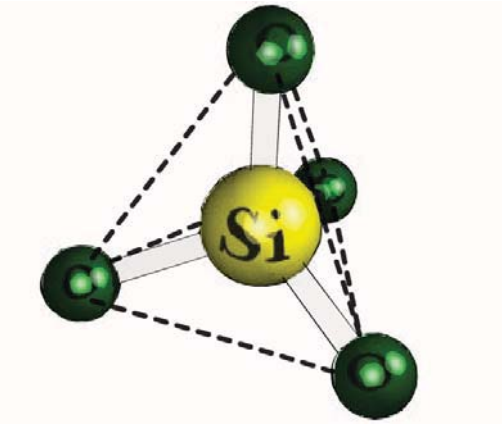

Figure 1.2: a schematic of three-dimensional tetrahedral arrangement in fused silica glass.

The distance between the neighboring oxygen ions is approximately 0.163 nm and 0.35 nm between two silicon ions [3]. This means that the glass structure is sparse and the space between the atoms can be filled with additional elements modifying properties of the glass. When these elements are added (e.g. rare-

earth ions) into the glass structure, the silicon-oxygen structure is opened up (figure 1.3) weakening the bond strength and lowering the fusion temperature and the viscosity either the density of the glass.

The germanium is commonly used to dope the silica glass during the core deposition process in the optical fiber. Thus the refractive index of the core was increased comparing to cladding glass. Here the silicon atom is replaced by germanium, where the tetrahedral structure is retained and its properties are similar to fused silica fiber [4].

Also, laser ions placed in glass have a larger fluorescent linewidth than in crystals. Furthermore, glasses have a good optical quality and they are comparatively easy fabrication compared to crystalline materials. On other hand, glass has a much lower thermal conductivity than most crystalline hosts [5].

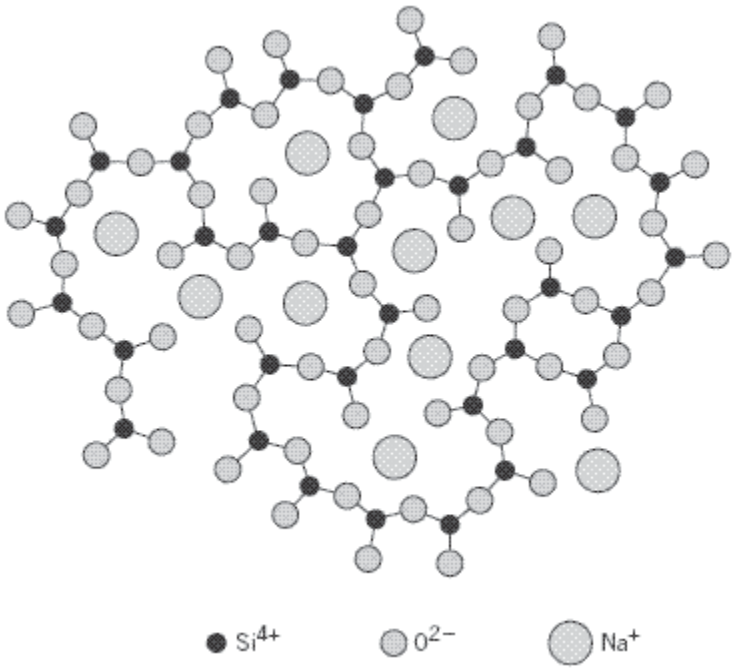

Figure 1.3: Schematic representations of ion positions in a sodium–silicate glass [7].

However, there are three classes of components for oxide glasses, the first one called glass network formers, where oxides have ability to form glass by themselves (SiO_2, GeO_2, B_2O_3 or P_2O_5). They form a 3-dimensional network with oxygen and so providing the very strong covalent bonds. On the other hand, the network modifiers such as Li_2O, K_2O and Na_2O alter the network structure; they are usually present as ions, compensated by nearby non-bridging oxygen atoms, bound by one covalent bond to the glass network and holding one negative charge to compensate for the positive ion nearby. The structure of

Na_2O-Si_2O_2 is shown in figure 1.5. Another group of oxides called intermediate oxides (TiO_2, AlO_2, ZrO_2 and BeO) can act as both network formers and modifiers, according to the glass composition. Some elements can play multiple roles; e.g. lead play as a network former (Pb^{4+} replacing Si^{4+}), or as a modifier [6].

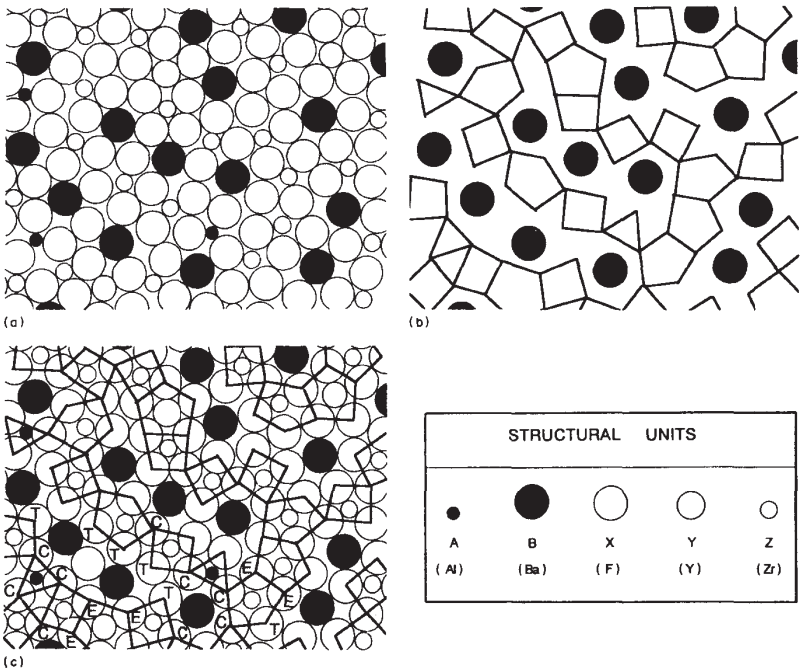

Figure 1.4: Schematic representation of a fluoride glass: (a) random close-packed model, (b) network model, (c) relation between a and b [11].

Another family of glasses is heavy metal fluoride glasses HMFG, which based on zirconium fluoride and indium fluoride. The most popular type of HMFG is ZBLAN (ZrF_4-BaF_2-LaF_3-AlF_3-NaF) composition, which is the most stable so far for fiber production and also the most resistant to crystallization under optical fiber perform-making and pulling conditions [8]. The fluoride glasses show worse mechanical, thermal, and chemical stability compared to SiO_2, which is consistent due the reduce bond strengths. In contrast to oxide glasses, the bonding of HMFG is not covalent but ionic, and much weaker. However, HMFGs have unique properties regarding refractive index and dispersion which make them of interest for specialized optical components. The refractive indices of HMFGs lie in the range 1.47-1.54 and are therefore comparable with many multicomponent oxide glasses [9]. The addition of heavy polarizable fluorides increases the index and lighter, less polarizable materials reduce it. Thus, in optical waveguides can therefore difference the refractive index between core and cladding by doping the core with PbF_2 or by ensuring an

excess of NaF, AlF_3 or HfF_4 in the cladding [10]. The structure of ZBLAN, which made from the fluorides of zirconium, barium, lanthanum, aluminum and sodium, is more complex than that of SiO_2. Two main models of complex glass matrices and their detailed description are given in [11]. Schematic representation of the fluoride glass is shown in figure 1.4; where for ZBLAN glass the Y atom can be replaced with La [6]. Here, Zr and Al are network formers, while La plays here the role of former, and Ba either Na are network modifiers.

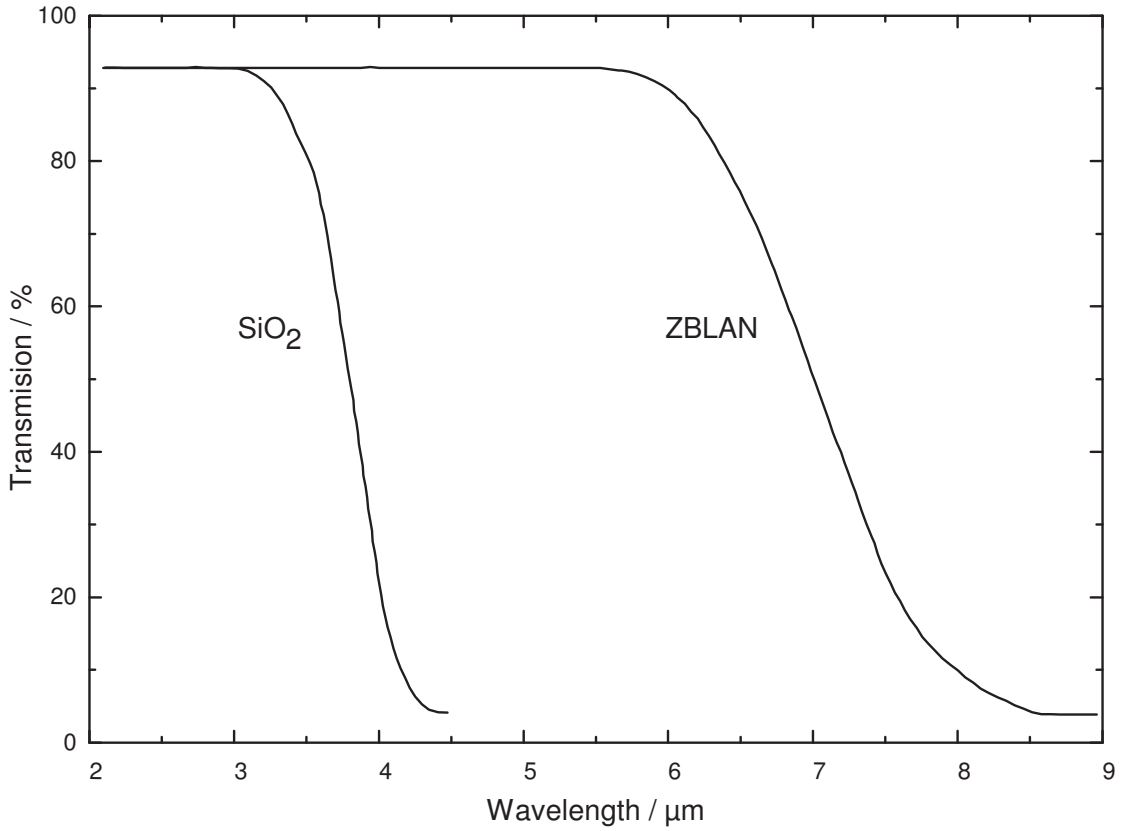

Figure 1.5: Infrared transmission spectra of silica and ZBLAN, thickness=5 mm [14].

In addition to the ionic bonds in ZBLAN glass it is clearly that its structure is much denser than that of SiO_2. But more fundamentally, the fluoride ion packing fractions are much higher than those of oxide ion in silicates. For example fluoride ions occupy 0.57 of the available space in ZBLAN glass whereas in vitreous silica oxide ions fill only 0.44 of the volume [12].Furthermore, the phonon energy for the vibrations in the glass matrix decreased by increased the atomic mass. Since the long and strong bonds between the atoms lead to high phonon energy, the SiO_2 has the highest phonon energy, which reaches to about 1050 cm^{-1}. Otherwise, the phonon energy reduced to about 55 % in ZBLAN glass. This is the reason for a better infrared transparency, which reached up to more 7 µm in ZBLAN glasses than just 2.5 µm for silicate glasses [13]

(figure 1.5). So the wide range optical transparency makes the HMFGs ideal candidates for the fiber amplifier or laser.

Moreover, the IR transparency of the optical material is limited by IR multiphonon absorption edge. In the multicomponent material masses and interatomic bonding forces are in charge of location, steepness, and changing of this edge. To simplification the fundamental phonon frequency w for the stretching vibrations of individual cation-anion pairs in a substance has been approximated by the relation [8]:

$$w = \frac{1}{2\pi c}\left(\frac{F}{\mu}\right)^{1/2}$$

where: F is the restoring force or force constant between the two ions of mass m_1 and m_2, where this constant is two times larger for silica glass than ZBLAN glass. While μ is the reduced mass defined by $m_1m_2/(m_1+m_2)$. It is obvious that the fundamental vibration frequency decreased with increasing reduced mass and with decreasing strength of the interatomic bond given by the force constant F. So the glass with the heavier atomic weight will exhibit a lower multiphonon absorption, where more than one phonon will be needed to bridge the difference in the energy states. Also it is expected in this HMFGs that lifetimes of the excited levels are longer than in silicate, which lead to existence more metastable levels and higher quantum efficiency. Thus, the absorptions from the excited states are more efficient.

Based on the above, HMFGs can be used for optimal optical pumping, such as Pr^{3+}/Yb^{3+} doped ZBLAN fiber laser. However, the microhardness value for fluoride glasses are about half of SiO_2, which is consistent with the reduced bond strengths. As a result fluoride glasses are likely to be less hard and more susceptible to handling damage.

1.3 Optical fiber losses

When the light flows through the fiber, it suffers optical attenuation due to a variety of mechanisms. Attenuation varies depending on the fiber type and the operating wavelength. Otherwise, fiber attenuation is caused by various mechanisms such as Rayleigh scattering, absorption and imperfections, as shown in figure 1.6.

The absorption losses are divided into intrinsic an extrinsic absorptions. The second one is related to losses caused by impurities within the silica such as illustrated in figure 1.6, where the two absorption peaks around 1240 and 1380 nm are primarily due to traces of OH^- ions. Therefore, the amount of water (OH^-) impurities in a fiber should be less than a few parts per billion. If these impurities are completely removed, the two absorption peaks disappear. Additionally, a strong absorption will happen in the wavelength range 0.8-1.6 µm by metal impurities, which are introduced into the fiber during fabrication. Here electronic transitions from one energy level to another occur in these metal ions. However, the intrinsic absorption losses are unavoidable, because they depend on the basic fiber-material properties. Figure 1.6 shows also the level of attenuation at the wavelengths of operation between two intrinsic absorption regions, which are the ultraviolet region (below 400 nm wavelength), and the infrared region (above 2000 nm wavelength).

Basically, the absorption in the ultraviolet region occurs when a light particle (photon) interacts with an electron system and excites it to a higher energy level. Generally, experimental data show that the attenuation caused by electronic absorption process decreases exponentially with increasing wavelength [8]. While the main cause of intrinsic absorption in the infrared region is the characteristic vibration frequency of atomic bonds especially silicon-oxygen (Si-O) bonds. Then the interaction between the vibrating bond and the electromagnetic field of the optical signal causes this infrared absorption.

Another process contributing to the intrinsic loss is scattering, where the Rayleigh scattering is the main loss mechanisms between the ultraviolet and infrared regions. Rayleigh scattering loss is caused by the interaction of light with density fluctuations within a fiber on a scale smaller than the optical wavelength λ. During fiber fabrication density changes are produced, since silica molecules move randomly in the molten state and freeze in place. The Rayleigh scattering loss α_R varies as $C\lambda^{-4}$, i. e., shorter wavelengths scatter more than longer wavelengths. The constant C is typically 1 $dBkm^{-1}\mu m^4$ correspond to α_R =0.12-0.16 dB/km at 1.55 µm.

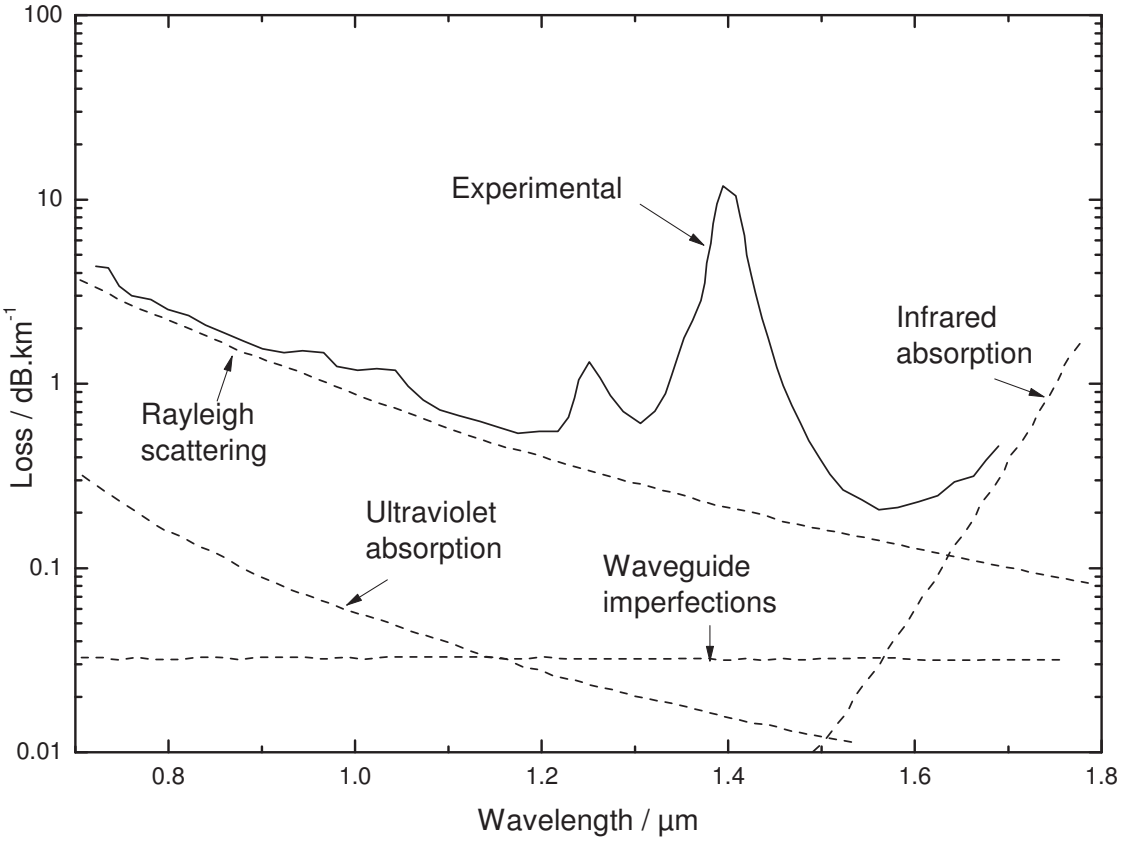

Figure 1.6: Contribution of various mechanisms to the spectral loss of optical fiber [15].

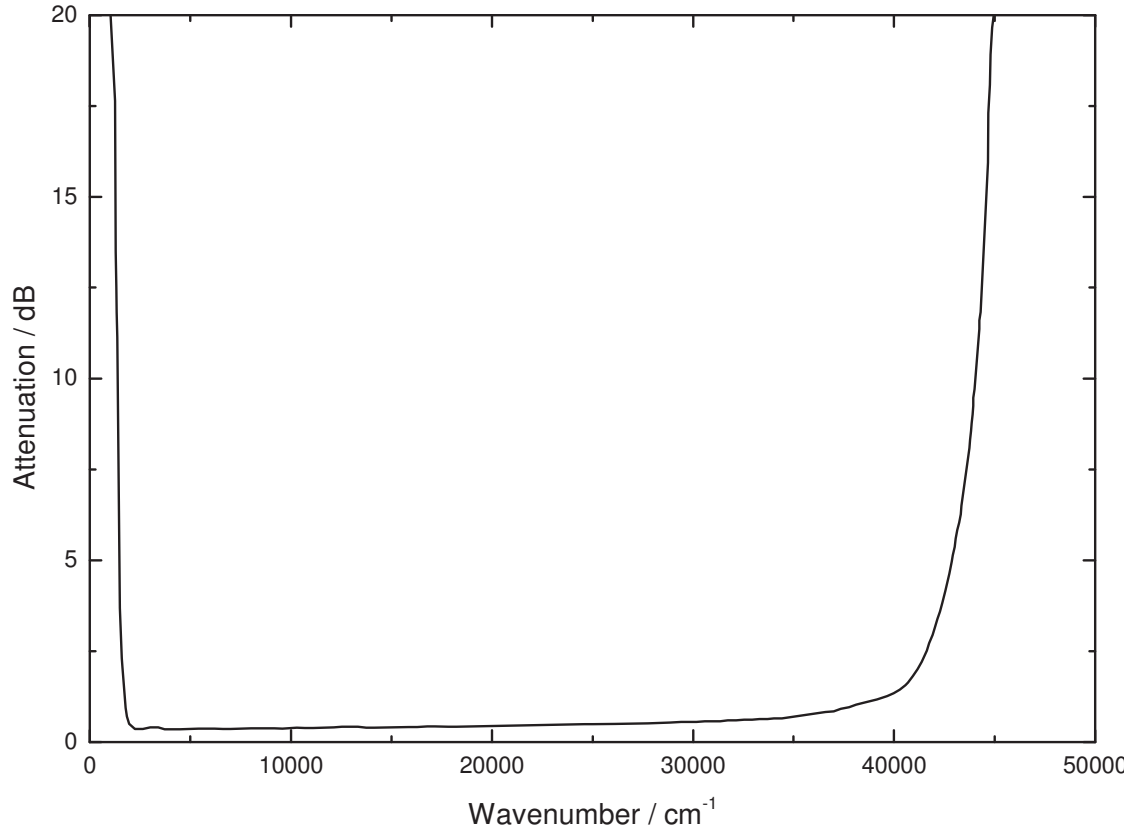

Figure 1.7: Transmission window of ZBLAN glass. Sample length 8.30±0.10 mm [16].

The theoretical contribution of Rayleigh scattering is reduced to below 0.01 dB/km for wavelengths longer than 3 µm. Figure 1.7 illustrated attenuation spectrum of the undoped ZBLAN glass, since infrared absorption in silica fibers begins to dominate the fiber loss beyond 1.6 µm. In figure 1.7 the thickness of used sample was 8.3 mm, in this case, the attenuation due to Rayleigh scattering should be about 0.005 dB at 50000 cm^{-1}, therefore the Rayleigh scattering should not be visible in such a thin glass [16]. In ZBLAN glass the infrared edge begins at about 2000 cm^{-1} (5 µm) and around 45000 cm^{-1} (220 nm) closed the window at the ultraviolet edge.

Finally, when index inhomogeneities on a scale longer than the optical wavelength, also the imperfection at the core-cladding interface as well as random core-radius variations can lead to additional losses called waveguide imperfections.

1.4 Rare earth doped fiber

Many applications, including laser projection displays, optical data storage, reprographics, biology, semiconductor manufacture and inspection, and medicine benefit from the availability of completely solid state lasers operating in the visible and UV spectral regions. Rare earth doped fluoride fibers may be used as such lasers. They have advantages compared to their gas or dye counterparts. In general, the fiber does not require thermoelectric or water cooling, because the cross-sectional area of the fiber is sufficiently small that heat is rapidly transferred from the pumped core region to the cladding and into the surrounding air. Moreover, fiber lasers are more efficient, compact, robust, less expensive, and have considerably longer lifetimes than gas or other solid state lasers. Additionally they often exhibit lower-output power noise than them.

The rare earths are a series of fifteen elements beginning with lanthanum, atomic number 57, and ending with lutetium, atomic number 71. They have a similar chemistry structure, which based on the gradual filling of the 4f subshell along the series [17]. All the elements have the configuration $4s^2$, $4p^6$, $4d^{10}$, $4f^x$, $5s^2$, $5p^6$, $5d^y$, $6s^2$, where represent closed shells for these levels, x=0 to 14 and y=0 or 1 [4, 18-19]. When the rare earths are incorporated into glass, they break up the covalently bonded glass structure, and the oxygen atoms, which are non-bridging, compensate charge within network [20].

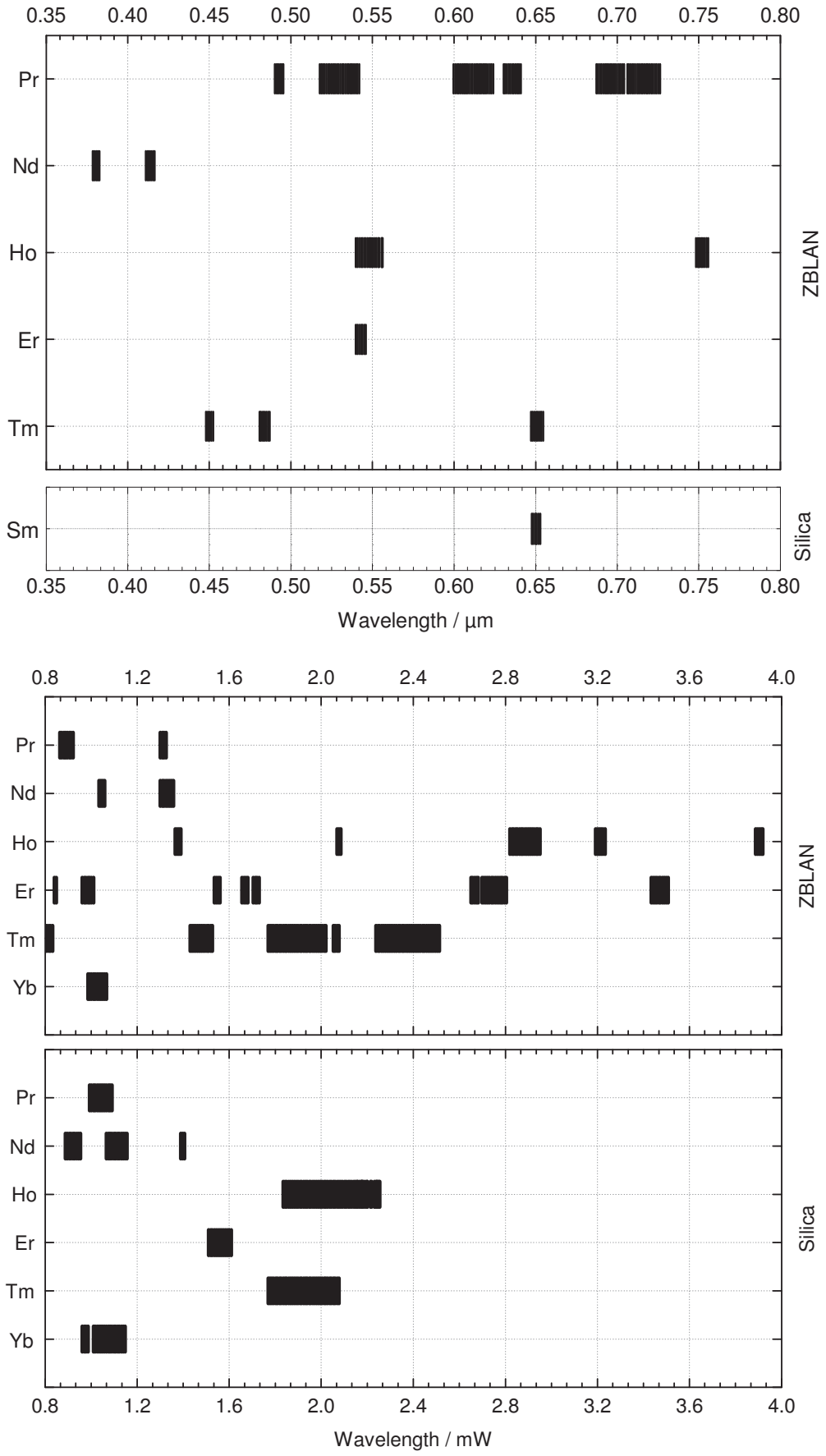

Figure 1.8: Wavelengths of infrared and visible either near-ultraviolet laser transitions demonstrated in rare earth doped ZBLAN and silica fiber [24].

However, the homogeneity of rare-earth ions in glasses depends very much on the host structure [21]. As example, the doping of rare-earth elements in the fluoride framework reaches up to 10 mol% [22], while in silica fiber is usually less than 0.1 mol% [23]. If this doping ratio increases to more than 0.1 mol% in a silica glass network, the doping ions will tend to cluster, because the silica glass does not accept well these doping ions, and consequently, the SiO_2 is distorted. Therefore, SiO_2 can incorporate only very small amounts of rare-earth are dopant before microscopic clustering occurs and ion-ion interactions shorten the fluorescence lifetimes. Otherwise, fluoride fiber lasers offer a wider range of wavelengths comparing with silica fiber lasers, where spanning the spectral range from approximately 0.4 to 4 µm. The most common fluoride glass used for the fabrication of fluoride fiber lasers is ZBLAN, therefore, figurer 1.8 illustrates the impact of the characteristics of ZBLAN on its utility as a host for visible an IR lasers, respectively, by providing a comparison between the laser transitions demonstrated in rare-earth doped ZBLAN fibers and silica fibers.

1.5 Faser laser

Due to the large absorption bandwidth for the absorption bands of rare-earth ions (typically >5 nm) broad-linewidth, pump sources can be used and pump wavelength stabilization is not required. Moreover, the confinement of both the pump and signal within the fiber core over the long distances is available with this kind of fiber lasers and makes its devices quite efficient. Consequently, increasing the fiber length can increase the attainable fiber laser power; provided that sufficient pump power can be coupled into the fiber core to fully pump the available gain volume. Also, with a small core diameter and high numerical aperture, high pump intensities are achievable even with modest pump powers.

However, visible fluoride fiber lasers are similar to silica fiber lasers in the sense that they consist of a relatively simple optical cavity and, as an example, dielectric mirrors coated directly onto the fiber end facets.